https://doi.org/10.5194/hess-2021-390
Preprint. Discussion started: 30 July 2021

Hydrology and Earth System Sciences
Discussions

Modelling groundwater recharge, actual evaporation and transpiration in semi-arid sites of the Lake Chad Basin: The role of soil and vegetation on groundwater recharge

Christoph Neukum[1], Angela Gabriela Morales Santos[2], Melanie Ronelngar[3], Sara Ines Vassolo[1]

[1] Federal Institute for Geosciences and Natural Resources, Hannover, 30655, Germany
[2] Institute for Soil Physics and Rural Water Management (SoPhy), University of Natural Resources and Life Sciences, Vienna, 1180, Austria
[3] Federal Institute for Geosciences and Natural Resources, Ndjamena, Chad

Correspondence to: Christoph Neukum (christoph.neukum@bgr.de)

Abstract.

The Lake Chad Basin, located in the center of North Africa, is characterized by strong climate seasonality with a pronounced short annual precipitation period and high potential evapotranspiration. Groundwater is an essential source for drinking water supply as well as for agriculture and groundwater related ecosystems. Thus, assessment of groundwater recharge is very important although difficult, because of the strong effects of evaporation and transpiration as well as limited available data.

A simple, generalized approach, which requires only a small number of field data, freely available remote sensing data, and well-established concepts and models, is tested for assessing groundwater recharge in the southern part of the basin. This work uses the FAO-dual K_c concept to estimate E and T coefficients at six locations that differ in soil texture, climate, and vegetation conditions. Measured values of soil water content and chloride concentrations along vertical soil profiles at these locations together with different scenarios for E and T partitioning and a Bayesian calibration approach are used to numerically simulate water flow and chloride transport. Average potential groundwater recharges and the associated model uncertainty at the six locations are assessed for the time-period 2003-2016.

Model results show that interannual variability of groundwater recharge is generally higher than the uncertainty of the modelled groundwater recharge. Furthermore, the soil moisture dynamics at all locations are limited by water availability for evaporation in the uppermost part of the soil and by water uptake in the root zone rather than by the reference evapotranspiration.

1 Introduction

The Lake Chad Basin (LCB) is one of the largest endorheic basins of the world with an area of approx. 2.5 million km². The basin covers parts of Algeria, Cameroon, Central African Republic, Chad, Libya, Niger, Nigeria and Sudan. According to the Lake Chad Basin Commission (LCBC, 2012), 45 million inhabitants are settled in the basin. The study areas Salamat and Waza Logone are located in the southern part of the LCB, along the major tributary river to the Lake Chad (Figure 1), the Chari-Logone river system, which accounts for around 80-90% of the Lake Chad inflow (Bouchez et al., 2016).

https://doi.org/10.5194/hess-2021-390
Preprint. Discussion started: 30 July 2021

Hydrology and Earth System Sciences
Discussions

Groundwater is an important source for drinking water supply as well as for agriculture and groundwater related ecosystems in the LCB. The Lake Chad, the rivers and the floodplains of the major rivers are characterized by strong seasonality, due to a pronounced short annual precipitation period and high potential evapotranspiration. Groundwater recharge, evaporation, transpiration, and the entire hydrological budget depend strongly on seasonality. However, the impact of transpiration as a potentially significant process of the hydrological budget (Jasechko et al., 2013,) has so far rarely been taken into account (Bouchez et al., 2016).

Many hydrological studies were published concerning the hydrological behaviour and budget of the Lake Chad, due to its substantial and frequent open water surface changes and related consequences to the population and the environment (e.g. Bouchez et al., 2016; Lemoalle et al., 2012; Olivry et al., 1996; Vuillaume, 1981). Another important topic associated to Lake Chad is groundwater recharge by infiltration of lake water into the Quaternary aquifer, which was estimated by isotopes studies (Fontes et al., 1969; Fontes et al., 1970; Gaultier, 2004; Zairi, 2008), by water and salt budgets (Bader et al., 2011; Carmouze, 1972; Roche, 1980) or hydrogeological models (Isihoro et al., 1996; Leblanc, 2002). Local scale studies focusing on the hydrological processes in the vadose zone are largely missing in the LCB. Recently Tewolde et al. (2019) published a local scale study using stable isotope and chloride concentrations in partly the same soil profiles used in this work.

For vadose zone studies, partitioning evapotranspiration (ET) into its respective soil evaporation (E) and plant transpiration (T) components is crucial for process-based understanding of fluxes (Anderson et al., 2017). There are a number of measurement and modelling approaches that can be used to estimate E and T separately. Some of the measurements include micro-lysimeter, soil heat pulse probes, Bowen ratio, and Eddy covariance to determine E; and sap flow, chambers, and biomass-transpiration relationship to measure T (Kool et al., 2014). Evapotranspiration partitioning can also be estimated directly by using stable isotopes to assess the ratio between E and T (Wu et al. 2016). Stable isotopes were used in combination with Eddy covariance on semi-arid environments as well (Aouade et al., 2016).

Anderson et al. (2017) reviewed some recent methodological developments for partitioning ET. These include micrometeorological approaches involving the flux variance partitioning of high-frequency Eddy covariance observations (Scanlon and Sahu, 2008, Palatella et al., 2014) and proxies for photosynthesis and transpiration such as measurements of isotopic fractionation (Griffis et al., 2010) and carbonyl sulfide uptake (Wohlfahrt et al., 2012). They also discussed the partitioning of energy balance between canopy and soil using remote sensing (Colaizzi et al., 2012; French et al., 2015).

The Food and Agricultural Organization of the United Nations (FAO) published a model (Allen et al., 1998) that uses an empirically defined crop coefficient (Kc) in combination with a reference ET (ET_0) to calculate crop evapotranspiration (ETc). There are two approaches for this method: single coefficient and dual crop coefficient. The FAO-dual Kc model is a validated method for ET partitioning and the most commonly applied (Kool et al. 2014). It has been widely used with good results for numerous crops under different conditions: e.g. wheat and maize in semi-arid regions (Shahrokhnia and Sepaskhah, 2013), wheat in humid climate (Vieira et al., 2016), cherry trees in temperate continental monsoon climate (Tong et al., 2016), irrigated eucalyptus (Alves et al., 2013), and canola in terrestrial climate (Majnooni-Heris et al., 2012).

https://doi.org/10.5194/hess-2021-390
Preprint. Discussion started: 30 July 2021


Hydrology and Earth System Sciences
Discussions

Quantification of water fluxes in the vadose zone and linking atmospheric water and solute input at the upper boundary of the soil with water and solute fluxes at different soil depths is frequently implemented using different kind of models. Numerical models need information on vadose zone properties for accurate parametrization to link fluxes with state variables such as unsaturated hydraulic conductivity and water retention curve. Estimation of effective soil hydraulic parameters, which are valid at the modelling scale, might be laborious. Furthermore, parameter estimation might vary significantly depending on the measurement method (Mertens et al., 2005), when water and solute fluxes dynamics are considered. Hydraulic and transport parameters obtained from inverse modelling can be ambiguous, if multiple parameters are simultaneously considered and boundary conditions are not well known. Combining different state variables of water flow and solute transport in one objective function was found to be a strategy for appropriate parametrization (Groh et al., 2018, Sprenger et al., 2015) and for the transient simulation of water and solute fluxes. However, large amount of data are necessary to obtain accurate estimates of state variables, which are rarely available in remote areas of Africa, and measurement of related variables are associated with a huge effort in such environments. Pedotransfer functions (PTF) bridge available and needed data and are frequently used to quantify soil parameters (van Looy et al., 2017; Vereecken et al., 2016). PTF strive to provide a balance between data accuracy and availability (Vereecken et al., 2016). Since PTF usually do not consider soil structure, they result better for homogeneous soils than for structured soils (Sprenger et al., 2015; Vereecken et al., 2010).

Recharge occurs even in the most arid regions, mainly due to concentration of surface flow and ponding with lateral and vertical infiltration (Lloyd, 1986). Direct recharge by precipitation is possible in semi-arid regions, but intermittently, owing to the fluctuations in the periodicity and volume of precipitation that is inherent to such regions (Lloyd, 2009). Scanlon et al. (2006) synthesized recharge estimates for semiarid and arid regions globally. They found that recharge is sensitive to land use and cover changes, hence management of such changes are necessary to control recharge. Moreover, they state that average recharge rates in semi-arid and arid regions range from 0.2 to 35 mm yr^{-1}, representing 0.1 to 5 % of long-term average annual precipitation. Edmunds et al. (2002) estimated direct recharge rates from precipitation in the Manga Grasslands in NE Nigeria (western LCB) at rates between 16 mm $year^{-1}$ and 30 mm yr^{-1}. Using the same method, they appraised the regional direct recharge for north Nigeria at 43 mm $year^{-1}$, which highlights the importance of infiltration from precipitation to the groundwater table at regional scale. Recently, Cuthbert et al. (2019) investigated the relationship between precipitation and recharge in sub-Saharan Africa using multidecadal hydrographs. They found that focused recharge predominates in arid areas and is mainly controlled by intense rainfall and flooding events. Intense precipitation, even during years of lower annual precipitation, results in some of the largest years of recharge in dry subtropical locations.

The Chloride Mass Balance (CMB) approach is a widely used technique for estimating groundwater recharge. Edmunds and Gaye (1994) used interstitial water chloride profiles from the unsaturated zone, in combination with measurements of chemical parameters from dug wells samples, to calculate groundwater recharge in the Sahel (mean annual rainfall 1970-1990 around 280 mm). A recharge rate of 13 mm $year^{-1}$ over the studied area was obtained. They conclude that it is an inexpensive technique, which can be applied in many arid and semi-arid areas. Tewolde et al. (2019) applied the CMB on soil profiles of the LCB, which are partly used in this study. They estimated generally lower annual recharge in Salamat (3 to 19 mm $year^{-1}$) compared

https://doi.org/10.5194/hess-2021-390
Preprint. Discussion started: 30 July 2021


Hydrology and Earth System Sciences
Discussions

to Waza Logone (50 to 118 mm year^{-1}). Among others, one major difficulty of CMB is the choice of a representative chloride concentration for soils, particularly those with a strong vertical chloride concentration variability.

In general, time series of relevant data for estimating groundwater recharge is scarce in the LCB. A simple, generalized approach, which requires only a small number of field data, freely available remote sensing data, and well-established concepts and models is tested for assessing groundwater recharge in the semi-arid part of the LCB. This work uses the FAO-dual K_c concept to estimate E and T coefficients at six locations, which differ in soil texture, climate, and vegetation conditions. Measured values of soil water content and chloride concentrations along vertical soil profiles at these locations are used together with different scenarios for E and T partitioning and a Bayesian calibration approach to numerically simulate water flow and chloride transport. Average potential groundwater recharges and the associated model uncertainty at the six locations are assessed for the time-period 2003-2016.

2 Data and methods

2.1 Study sites

The LCB is a Mesozoic basin and a major part of its geology comprises sedimentary formations from the Tertiary and Quaternary periods (LCBC, 1993). The Quaternary sediments form a continuous layer of fluviatile, lacustrine and aeolian sands. These medium to fine-grained sands act as an unconfined transboundary aquifer, as do the rest of the aquifers in the LCB, and are isolated from underlying aquifers by a thick layer of Pliocene clay (Leblanc et al., 2007; Vassolo, 2009). The Tertiary formation (Continental Terminal) consists of sandstones and argillaceous sands and is a classic example of a confined aquifer system that becomes artesian in the surroundings of the Lake Chad (Ngatcha et al., 2008). The availability of water from precipitation as well as the deposition characteristics of the aquifer play an important role in the aquifer recharge of the upper unconfined sands (Vassolo, 2009).

The study sites (Figure 1, Table 1) are located in the floodplains Waza Logone and Salamat in the southern Sahel subzone. In the Salamat region, millet and sorghum are grown with trees such as Acacia albida, A. scorpioides and A. sieberana present along the margins of the floodplains (Bernacsek et al., 1992). In the Waza Logone area, the vegetation is classified according to the duration of submersion, being the grass savannahs flooded for longer periods of time (Batello et al., 2004).

2.2 Climate data

Monthly precipitation and potential evapotranspiration data from 1970 to 2019 for the specific sites in Salamat and Waza Logone are extracted from the CRUTS 4 database (Harris et al. 2020). The potential evapotranspiration is calculated using the Penman-Monteith method and is considered herein as the reference evapotranspiration (ET_0). The wind speed values at 10 m above ground for Salamat and Waza Logone were obtained from Didane et al. (2017). To adjust these values for 2 m above ground, a correction factor of 0.7479 was applied, based on a logarithmic wind speed profile (Allen et al., 1998).

https://doi.org/10.5194/hess-2021-390
Preprint. Discussion started: 30 July 2021


Hydrology and Earth System Sciences
Discussions

Average annual precipitation in Salamat and Waza Logone are 807 mm and 709 mm, respectively. The rainy season is typically from May to September with maximum precipitations in July and August. Overall, Waza Logone presents higher ET_0 (169 mm $month^{-1}$) than Salamat (144 mm $month^{-1}$). Average annual values of ET_0 are 1718 mm in Salamat and 2011 mm in Waza Logone, exceeding annual precipitation by more than twice. However, during the peak of the rainy season (July to September) the monthly water balance is positive. The average water balance for July until September between 2003 and 2016 is 131 ± 101 mm $month^{-1}$ and 90 ± 63 mm $month^{-1}$ for Salamat and Waza Logone, respectively (Figure 2).

Chloride concentration of precipitation were measured in 42 samples collected in N'Djamena and Waza-Logone areas between 2014 and 2020 for different precipitation events and stages of the rainy season. The precipitation was sampled using a Hellmann rainwater collector in N'Djamena. Average chloride concentration in May is 2.5 ± 2.3 mg/l (3 samples). Precipitation in June to September have suggestively lower chloride concentrations declining from 0.6 ± 0.3 mg/l to 0.26 ± 0.12 mg /l and 0.38 ± 0.14 mg/l at the end of the season. Strong rain events in July and August have chloride concentrations between 0.2 and 0.3 mg/l. The annual wet Chloride deposition sums to 1.8 ± 0.2 kg/ha. Dry deposition of chloride is estimated between 10 – 30% of wet deposition (Bouchez et al. 2019). The measured values are in the range of published data (Goni et al. 2001, Gebru and Tesfahunegn, 2019). However, not all rain samples could be analyzed for chloride concentration, due to limited sample amount. This is particular true for minor events with low precipitation amounts at the very beginning of the rainy season.

2.3 Soil and vegetation data

At each study site, vertical soil profiles are drilled using a hand auger. In Salamat, soil profiles were sampled in 2016 and 2019. In Waza Logone soil samples were sampled in 2017 only, due to security reasons in 2019. Each of the soil profiles were fractionated into 10 cm intervals and filled into headspace glass vials and plastic bags. Each soil fraction was tested for grain size distribution using sieving and sedimentation standard procedures, resident chloride concentration, and gravimetric water content. Chloride concentration was analyzed after aqueous extraction from oven dried (105°C for 24 hours) soil samples in the plastic bags following the standard guideline DIN EN 12457-1 (Tewolde, 2017). The gravimetric water content was converted into volumetric water content using typical bulk densities for the different soil types and locations (Global Soil Data Task Group, 2000). The type of vegetation and the annual cycle of crops, length of the flooding period, and vegetation throughout the dry period were mapped during field work and documented by surveying resident population. In addition, MODIS vegetation indices data (Didan, 2015) were used to justify the documented annual cycle of phenology (Figure 3).

2.4 Partitioning of evaporation and transpiration

The calculation of reference evapotranspiration ET_0 as well as crop evapotranspiration (ET_c) and its partitioning into potential evaporation and transpiration is based on the dual crop coefficient (Kc) method (Allen et al., 1998). The approach requires two different coefficients the basal crop coefficient (Kcb) that describes plant transpiration and the soil water evaporation coefficient (Ke) that depicts evaporation from the soil surface. Kcb is defined as the ratio of the crop evapotranspiration over the reference evapotranspiration (ET_c/ET_0), when the soil surface is dry and transpiration occurs at a potential rate (i.e., water

https://doi.org/10.5194/hess-2021-390
Preprint. Discussion started: 30 July 2021


Hydrology and Earth System Sciences
Discussions

does not limit transpiration). Ke describes the evaporation component of ET_c. When the topsoil is wet, Ke is maximal, but diminishes with drying out of topsoil to become zero, if no water remains near the soil surface for evaporation. The so-called dual Kc is the sum of Kcb and Ke. The parameters required for the estimation of ET_c are the reference evapotranspiration (ET_0), the basal crop coefficient (Kcb) and the evaporation coefficient (Ke):

$$ET_c = ET_0 * K_c = ET_0 * (K_{cb} + K_e)\,, \quad (2)$$

Onsite information on vegetation and phenology, such as month of planting, full emergence of crop, and harvesting was used to define the monthly variation of vegetation at the study sites. These different vegetation periods were combined with crop specific Kcb information for sorghum and grass provided in Allen et al. (1998). Following Allen et al. (1998), the coefficients Kcb−mid and Kcb−end were adjusted to comply with the local semi-arid climate in Salamat and Waza Lagone. Monthly Kcb values for acacia were estimated based on the work of Do and Rocheteau (2003) and Do et al. (2008).
Site-specific estimated monthly variation of ground cover and flooding periods with ranges of crop coefficient (Kcb), soil water evaporation coefficient (Ke), and root depth is provided in Table S1.

2.5 Modelling water flow and solute transport

2.5.1 Model concept, setup, and initial conditions

The chloride profiles measured in soil represent the input history for water and solute budget from past precipitation events, which can be estimated by transient water flow and solute transport modelling. The model concept assumes that atmospheric chloride input is restricted to solute in precipitation and that the chloride concentration profile results from solute enrichment in the soil, due to evaporation and transpiration. A precise parametrization of the unsaturated flow and transport model and a robust quantification of groundwater recharge are not possible with the available data and hence cannot be the scope of this study. However, the model results estimates groundwater recharge magnitude and variability based on information regarding soil texture and vegetation as well as associated results uncertainty. This approach is appropriate for locations with limited availability of long-term soil water measurements.
The Hydrus-1D software package was used to simulate transient water flow and solute transport in the six variably saturated soil profiles. Hydrus-1D numerically solves the Richards (1931) equation for variably-saturated water flow and advection-dispersion equations for heat and solute transport (Šimůnek et. al, 2009). The processes simulated in the six soils were water flow, solute transport, and root water uptake for a defined period subdivided in monthly steps. The calculations ended at the soil sampling time (December 2016 and July 2019 for Salamat and June 2017 for Waza Logone). Root growth was considered in all the profiles except for ST2, in which the roots of the acacia trees were distributed along the whole profile and assumed invariant over the simulation period. Because the initial conditions of soil moisture and resident chloride concentration are unknown, arbitrary values were adopted. To account for the different residence times of water and chloride, due to different degrees of evapotranspiration and unknown initial conditions, the models encompass different calculation time periods: ST1, ST2, WL1 and WL2 start in 1990 whereas ST3 in 2010 and WL3 in 1970. To adequately estimate the initial conditions and

https://doi.org/10.5194/hess-2021-390
Preprint. Discussion started: 30 July 2021


Hydrology and Earth System Sciences
Discussions

reduce the computation time for calibration, a burn-in period of 80 years was considered for ST1 and ST2. All profiles were discretized into 101 nodes and different horizons according to the soils types interpreted from the individual grain size distributions.

2.5.2 Water flow

For calculation of water retention and unsaturated hydraulic conductivity functions, the Mualem-van Genuchten (MVG) model (van Genuchten, 1980) was applied. The initial parametrization of these functions was realized using pedotransfer functions implemented in Rosetta (Schaap et al., 2001), which is a dynamically linked library coupled to Hydrus-1D. The input parameters for each profile were the percentages of sand, silt, clay, and bulk density at several depths. Whenever several consecutive layers of a profile showed almost the same grain distribution (texture), the layers were lumped in one, parameter averages were used in the model, and the measured soil moisture profiles were considered indicatively. The tortuosity parameter l [-] of the MVG was set to 0.5 in accordance to Mualem (1976).
The upper boundary condition was defined as variable atmospheric condition with surface runoff, whereas the lower boundary condition was set to zero-gradient with free drainage of water for all profiles, except WL3. At WL3 confined groundwater conditions prevailed below the confining clay layer encountered at 3.9 m depth. Groundwater was hit at 3.9 m depth, but rapidly rose to 2.6 m below surface. Consequently, a constant head condition was implemented at that depth.

2.5.3 Root water uptake and root growth

The sink term S in the Richards equation, defined by Feddes et al. (1978) as the volume of water removed from a unit volume of soil per unit time due to plant water uptake, was considered in all soil profiles according to the prevailing vegetation (Table S1). The Feddes' default parameters for grass were used in ST03 and Waza Logone profiles. In ST01, corn parameters were selected, since sorghum data is not available. Sorghum and corn roots extract water from approximately the same soil depths and have similar average root density distribution, in comparison with other crops, e.g. soybeans (Righes, 1980). In the case of acacia in ST2, the adopted parameters correspond to deciduous trees.
For sorghum in ST1, an average root depth of 1 m was adopted for the initial and end seasons, and 2 m for development and mid seasons. In ST3 and WL2, the vegetation was defined as grass, while in WL1 and WL3 as grasslands with a flooding period. Rooting depths values used in these sites range from 0.1 to 0.5, depending on the growth stage of grass. Monthly variations were specified as time variable boundary conditions. The median maximum rooting depth value of annual grass in water-limited ecosystems is 0.37 m with a 95 % of confidence in an interval of 0.26-0.55 m (Schenk and Jackson, 2002).
For ST2, the root depth of the acacia tree was considered to be constant over the simulation time with maximum root distribution at 0.5 m and decreasing distribution down to 2 m (Beyer et al., 2016).

https://doi.org/10.5194/hess-2021-390
Preprint. Discussion started: 30 July 2021

Hydrology and Earth System Sciences
Discussions

2.5.4 Solute transport

The chloride concentration in soil water was simulated using an equilibrium advection-dispersion model implemented in Hydrus1-D. Hydrodynamic dispersion was implemented considering dispersivity values of 10 % of the individual layer thickness in the soil model, a molecular diffusion coefficient of 1.3 x 10^{-9} m^2s^{-1}, and a tortuosity factor as defined by Millington and Quirk (1961). Adopted dispersivity values are with the reported ranges between 0.8 cm and 20 cm (Vanderborght and Vereecken 2007, Stumpp et al, 2009, 2012).

A third type (Cauchy) boundary condition was applied to the upper and a zero-gradient boundary condition to the lower boundary. The transient liquid phase concentration of the infiltrating water follows measured chloride concentration in precipitation sampled in N'Djamena. Chloride concentration of ponding water in Salamat ranges between 2.5 mg/l and 25 mg/l with an average of 9 mg/l (n=4).

2.5.5 Crop evapotranspiration scenario definition

Simulated crop evaporation scenarios and their individual descriptions are provided in Table 2. Parameter ranges for minimum, maximum Kcb and Ke factors are listed in Table S1. The average corresponds to the average value calculated from minimum and maximum factors.

2.5.6 Bayesian model calibration

Based on the crop evapotranspiration scenarios, the models were calibrated using a Bayesian calibration referenced by the soil moisture and chloride concentration profiles. We implemented the sum of likelihood functions for soil moisture and chloride concentration to calculate the log-likelihood of a simulation given the observations and standard deviations at each calibration step. The posteriori parameter distribution was estimated using the Differential Evolution Markov Chain Monte-Carlo (DEzs) algorithm with three sub-chains (ter Braak and Vrugt, 2008) implemented in the R package BayesianTools (Hartig et al. 2019). The number of iterations was defined individually according to a Gelman-Rubin reduction factor < 1.2.

The calibration was implemented with scaling factors ranging from 0.75 to 1.25 for the MVG parameters saturated volumetric water content, alpha, and n individually as well as chloride concentration and transpiration to account for observed variabilities. However, ranges for MVG model parametern were constraint to n > 1.01. Log-transformed saturated hydraulic conductivity for each layer were considered with ranges from -0.5 to 0.5. The scaling factor for transpiration was used as divisor for evaporation simultaneously to remain within the calculated rate of ET_0. From all accepted model runs, 100 were randomly selected at each individual location to evaluate average model results and standard deviations.

https://doi.org/10.5194/hess-2021-390
Preprint. Discussion started: 30 July 2021

Hydrology and Earth System Sciences
Discussions

248 **3 Results**

249 **3.1 Grain size distribution**

250 Soil textures were defined based on grain size distributions of the six profiles (Figure 4) according to the US Department of
251 Agriculture soil texture triangle. Most of them are fine-grained soils (clay, sandy clay) and fine-grained soils with minor parts
252 sand and loam. Only soil profile ST03 is dominated by sand and sandy clay loam.

253 **3.2 Model parametrization**

254 The calibrated parametrization of the MVG model for each layer of the six sampling locations are plausible in general (Table
255 3). The posterior distributions of the Bayesian calibration show the sensitive parameters of the model fit. For ST1, these are
256 the model parameters n, saturated water content, chloride concentration, and the fraction of transpiration in evapotranspiration.
257 The saturated hydraulic conductivity is less sensitive (Fig. S1). For ST2, the sensitivities of the model parameters are similar
258 with the saturated hydraulic conductivity of the upper layer being sensitive and the influence of chloride concentration being
259 less significant (Fig. S2) compared to the other locations. The model fits of the data from site ST3 are generally insensitive.
260 Only the model parameters alpha, n, and saturated hydraulic conductivity of the upper layer and chloride concentration in
261 precipitation show tighter posteriori distributions (Fig. S3). For the model for site WL1, the model parameters n of layers 1, 2,
262 and 3 and as well as the saturated water content of layers 3 and 5, and subordinately of layer 4, are sensitive. The parameters
263 alpha for layers 1 to 5 and the chloride concentration and fraction of transpiration are hardly sensitive in the range of the prior
264 distribution (Fig. S4). For the model for WL2, the parameters n of all layers, the saturated hydraulic conductivity of layer 3,
265 and the saturated water content of layers 2 and 3 are sensitive (Fig. S5). For WL3, the saturated water contents of layer 2 and
266 as well as the saturated hydraulic conductivity of layers 1 and 2 and the fraction of transpiration in evapotranspiration are
267 sensitive (Fig. S6).
268

269 **3.3 Soil water content, chloride concentration and groundwater recharge**

270 Measured and simulated water content and chloride concentration profiles for individual scenarios are shown in Fig. 5. The
271 average root mean squared error (RMSE) of simulated water content for all individual scenarios ranges from 0.02 to 0.06
272 (Table 4). In general, the models reproduce well the water content and chloride concentrations. However, the misfit of
273 measured soil water content to simulated water content is considerable for the models ST1 and partly ST2. The models do not
274 represent the high chloride concentrations in the uppermost part of soil profiles for ST3, WL1, and WL2. The standard
275 deviations in chloride concentration of the randomly selected model runs are exceptionally high in the lower part of ST2 that
276 corresponds to the poor sensitivity of the chloride concentration at the upper boundary and the comparably wide range of
277 measured chloride concentration in ponding water in the Salamat region (2.5 – 25 mg/l).
278

https://doi.org/10.5194/hess-2021-390
Preprint. Discussion started: 30 July 2021


Hydrology and Earth System Sciences
Discussions

279 The interannual variability of modelled groundwater recharge differs considerably among locations (Figure 6, Table 5). In
280 general, interannual groundwater recharge variability depends on vegetation and soil texture with related water retention
281 capacity. Vegetation with deep roots on soil with comparably high water retention capacity have a higher interannual
282 variability, e.g. ST1, ST2 where recharge occurs only in years with high precipitation. Fine textured soils with shallow rooting
283 vegetation have an intermediate variability (WL1, WL2, and WL3), where years without recharge occur only during drought
284 periods. The coarser textured soils with grass cover has low interannual recharge variability (ST3) and recharge occurs each
285 year. Years with high precipitation, e.g. 2006, 2007, and 2008 in Waza Logone as well as 2010 in Salamat, produce strong
286 groundwater recharge.
287 The highest recharge was calculated for ST3 in Salamat, where on one hand water balance during the rainy season (July-
288 September) is higher compared to the Waza Logone region and on the other hand, shallow rooting vegetation on comparably
289 coarse soil texture with low water retention capacity and higher hydraulic conductivity prevail. The other locations in Salamat
290 have lower calculated annual recharge, due to deep rooting vegetation and higher soil water retention capacity. The impact of
291 soil texture on annual groundwater recharge becomes apparent by comparing the three location in Waza Logone with the same
292 vegetation on soils with different water retention capacities and hydraulic conductivities. In general, groundwater recharge
293 expressed as fraction of precipitation is below 8 % (Table 5). Only at ST3, a comparably high fraction of app. 12 % is estimated.
294
295 Chloride concentration and water budget of the soils over the modelled time-period are rather unstable and differ for the six
296 locations. At location ST2 with clay loam soil covered by Acacia and grass, accumulation of chloride takes place over several
297 years, due to the high transpiration related to the effective field capacity (Figure 7). However, in high precipitation periods,
298 most of the accumulated chloride is leached to groundwater and soil concentration diminishes. It should be noted that at this
299 site, the measured chloride concentrations cannot be reconstructed if only input via precipitation is considered. The measured
300 profile can only be plausibly modelled with an additional input via ponding water. Chloride input at the upper boundary is
301 consequently much higher at ST2 compared to the other locations considered in this study.
302 At location ST3, the chloride accumulation is much lower compared to the other locations. Chloride budget is controlled by
303 the fast groundwater recharge response to precipitation, which flushes chloride from the soil towards groundwater annually.
304 The majority of chloride infiltrated with precipitation remains in the vadose zone over years and is leached towards
305 groundwater mainly during years with precipitation or water infiltration above threshold values (Figure 7). Chloride
306 accumulation is highest in profiles with clay soils and high effective field capacity (ST1, WL1, and WL3).

307 **3.4 Evaporation and transpiration**

308 The transpiration amount depends on the availability of water in the root zone and the type of vegetation cover. At ST1, annual
309 transpiration presents two peaks: one related to sorghum and the other to grass (Figure 8). At each location and in every
310 simulation year, soil water content in the root zone reaches the wilting point defined by the specific parametrization of the root
311 water uptake model.

https://doi.org/10.5194/hess-2021-390
Preprint. Discussion started: 30 July 2021


Hydrology and Earth System Sciences
Discussions

312 The actual evaporation rate depends mainly on the availability of water in the upper soil zone (Table 6). Clay and clay-loam
313 with relatively high water storativity have larger amounts of evaporated water compared to sand and loam soils. During dry
314 seasons, the uppermost part of the soils dries up annually, which restricts evaporation strongly.
315 Actual evapotranspiration is lower than the reference evapotranspiration most of the year. During and shortly after the rainy
316 season, when sufficient soil water is available, actual evapotranspiration is comparable to or higher than ET_0 depending on the
317 vegetation.

318 **4 Discussion**

319 Soil texture information is helpful to limit possible MVG parameter ranges while searching for realistic parameter sets
320 (Sprenger et al. 2015). However, poor representation of soil moisture dynamic using MVG parameters derived with ROSETTA
321 are reported (Sprenger et al. 2015) and indications are given that soil structure has to be taken into account (Vereecken et al.
322 2010), especially for soils where high rock content influences water flow due to inherent heterogeneity (Sprenger et al. 2015).
323 The soils at the locations considered in this study belong to Quaternary sediments in the Lake Chad basin and heterogeneity,
324 due to rock fragments is largely absent. Furthermore, soil moisture dynamics over the year is much higher in soils of flooding
325 planes compared to soils from the more humid regions in the south, where precipitation although large occurs over 4-5 months
326 and lacks over the rest of the year. It is expected that high soil moisture dynamics, rather homogeneous soils, and the monthly
327 resolution of climate data result in minor impact of soil structure on MVG parametrization and groundwater recharge as shown
328 in chapter 3.2. Soil moisture dynamics at all locations considered in this study are limited by water availability for evaporation
329 in the uppermost part of the soil and by water uptake in the root zone, but not by the reference evapotranspiration. However,
330 time resolution of precipitation and evapotranspiration data is monthly and the models probably underestimate soil moisture
331 dynamics.
332 Calculated chloride concentrations for the soil profiles give indications of appropriate MVG parametrization as well as
333 evaporation and transpiration partitioning. However, uncertainty of chloride input and its transient variability in particular is
334 expressed in rather wide and partly bimodal distribution of the scaling factor (sc_Conc) included in the calibration (Figures
335 S1-S6 in supplement material). On one hand, measured chloride concentration in precipitation are in agreement with other
336 studies in central Africa (Goni et al. 2001, Gebru and Tesfahunegn, 2019) and its transient behavior within the rainy season is
337 considered in the applied model. On the other hand, impact of dry deposition is unknown, because of data scarcity and potential
338 lateral flow of periodical flooding. Furthermore, due to the monthly resolution of the atmospheric boundary condition, extreme
339 rain events that cause surface runoff cannot be reflected in the model. The variability of chloride concentration in some of the
340 soil profiles, which cannot be completely reproduced by the model, indicates either a higher variability of chloride input and/or
341 a larger variability in soil physics.
342 Bouchez et al. (2019) identified a chloride deficit between deposition and river export in the Chari-Logone river system of
343 88 % (only 12 % of the deposited chloride is exported via river water). They refer to the chemical memory effect, which can
344 play an important role in arid regions. Our simulations show the importance of the vadose zone for storage of chloride over

https://doi.org/10.5194/hess-2021-390
Preprint. Discussion started: 30 July 2021


Hydrology and Earth System Sciences
Discussions

longer periods of time, which explains on one hand the fate of chloride in the basin and confirms the chemical memory effect. In this context, it must be noted that the thickness of the vadose zone at the locations considered in this studies is between 4 and 21 m, where important amounts of chloride can be potentially stored leading to a strong delay of the chemical signal from precipitation to groundwater.

5 Conclusions

The quantitative estimation of groundwater recharge in the LCB is difficult, due to the scarce data availability and the expected low recharge quantities. Estimation of low recharge amounts in arid and semi-arid areas are usually ambiguous, because the immanent measurement inaccuracies lead to uncertainties during data processing and modelling. Quantification of water and solute fluxes in the vadose zone is often implemented using long-term time series of soil moisture, pressure heads, and concentration data in combination with appropriate models. Monitoring of soil moisture and solute concentration over longer periods at different depths and sites is difficult in the LCB, due to limited infrastructural prerequisites and challenging climatically boundary conditions. The presented approach combines soil moisture and chloride concentration quantified along vertical soil profiles in different locations within the LCB with numerical models and freely accessible data, while considering data uncertainty. Although modelling results of soil water content and chloride concentration deviate considerably from measured values for some profiles, their magnitudes agree largely. This is especially important for chloride concentration in the middle and deeper parts of the profiles, where seasonal effects are mainly averaged. Thus, the estimates of soil water balance and especially of groundwater recharge as well as the adopted soil physical parameters are plausible.

Groundwater recharge values estimated in this study are different to those published in Tewolde et al. (2019). This is due to the more extensive availability of chloride concentration data in precipitation available for this study. In addition, Tewolde et al. (2019) roughly estimated one value of saturated porosity for each profile. Because this parameter is rather sensitive in the Bayesian calibration, several values along each of the profiles were considered in this study. In contrast to the assessment of groundwater recharge with the chloride balance method (Tewolde et al. 2019), the method used here allows not only estimates of mean recharge, but also its interannual dynamics, variability, and the classification of the uncertainties of the input data and modelling. The interannual variability of groundwater recharge is generally higher than the uncertainty of the modelled groundwater recharge. The soil moisture dynamics at all locations considered in this study are limited by water availability for evaporation in the uppermost part of the soil and by water uptake in the root zone and not by the reference evapotranspiration. Upscaling of the results to larger areas must be interpreted with caution since the considered combinations of soils and vegetation probably do not cover all combinations present in Salamat and Waza Logone regions.

Author contribution

M.R. conducted fieldwork; A.G.M.S. and C.N. conducted modelling and interpretation; C.N. and S.V. design the study and conducted writing. All authors contributed to the discussion of results and commented the manuscript.

https://doi.org/10.5194/hess-2021-390
Preprint. Discussion started: 30 July 2021

Hydrology and Earth System Sciences
Discussions

Acknowledgement

This study was conducted within the framework of the technical cooperation project "Lake Chad Basin - Management of Groundwater Resources" jointly executed by the Lake Chad Basin Commission (LCBC) and the German Federal Institute for Geosciences and Natural Resources (BGR). The technical project is funded by the German Federal Ministry for Economic Cooperation and Development (BMZ).

References

Allen, R. G., Pereira, L. S., Dirk, R., and Smith, M.: Crop evapotranspiration: Guidelines for computing crop water requirements. FAO Irrigation and Drainage Paper No. 56. Rome, Italy. https://doi.org/10.1016/j.eja.2010.12.001, 1998.

Alves, M. E. B., Mantovani, E. C., Sediyama, G. C., & Neves, J. C. L. (2013). Estimate of the crop coefficient for Eucalyptus cultivated under irrigation during initial growth. Cerne, 19(2), 247–253. https://doi.org/10.1590/S0104-77602013000200008

Anderson, R. G., Zhang, X., and Skaggs, T. H.: Measurement and Partitioning of Evapotranspiration for Application to Vadose Zone Studies. Vadose Zone Journal, 16(13), 0. https://doi.org/10.2136/vzj2017.08.0155, 2017

Aouade, G., Ezzahar, J., Amenzou, N., Er-Raki, S., Benkaddour, A., Khabba, S., and Jarlan, L.: Combining stable isotopes, Eddy Covariance system and meteorological measurements for partitioning evapotranspiration, of winter wheat, into soil evaporation and plant transpiration in a semi-arid region. Agricultural Water Management, 177, 181–192. https://doi.org/10.1016/J.AGWAT.2016.07.021 , 2016.

Bader, J., Lemoalle, J., and Leblanc, M.: Modèle hydrologique du Lac Tchad, Hydrolog. Sci. J., 56, 411–425, 2011.

Batello, C., Marzot, M., and Harouna Touré, A.: The future is an ancient lake: Traditional knowledge, biodiversity and genetic resources for food and agriculture in the Lake Chad basin ecosystems. FAO Interdepartmental Working Group on Biological Diversity for Food and Agriculture, Rome, 2004.

Bernacsek, G. M., Hughes, J. S., and Hughes, R. H. (Ed.): A directory of African wetlands. International Union for the Conservation of Nature and Natural Resources, 1992.

Beyer, M., Koeniger, P., and Himmelsbach, T.: Constraining water uptake depths in semi-arid environments using stable water isotopes Results & Discussion. https://doi.org/10.5281/zenodo.56159, 2016.

Bouchez, C, Deschamps P., Goncalves J, Hamelin B, Nour AM, Vallet-Coulomb C & Sylvestre F: Water transit time and active recharge in the Sahel inferred by bomb-produced 36Cl. Nature, scientific reports, 9: 7465, (2019).

Bouchez, C., Goncalves, J., Deschamps, P., Vallet-Coulomb, C., Hamelin, B., Doumnang, J.C., Sylvestre, F.: Hydrological, chemical, and isotopic budgets of Lake Chad: a quantitative assessment of evaporation, transpiration and infiltration fluxes, Hydrol. Earth Syst. Sci., 20, 1599–1619, 2016.

Carmouze, J.-P.: Originalité de la régulation saline du lac Tchad, Comptes Rendus de l'Académie des Sciences. Série D: Sciences Naturelles, 275, 1871–1874, 1972.

https://doi.org/10.5194/hess-2021-390
Preprint. Discussion started: 30 July 2021

Colaizzi, P. D., Kustas, W. P., Anderson, M. C., Agam, N., Tolk, J. A., Evett, S. R., … O'Shaughnessy, S. A.: Two-source energy balance model estimates of evapotranspiration using component and composite surface temperatures. Advances in Water Resources, 50, 134–151. https://doi.org/10.1016/j.advwatres.2012.06.004, 2012.

Cuthbert, M. O., Taylor, R.G., Favreau, G. et al.: Observed controls on resilience of groundwater to climate variability in sub-Saharan Africa. Nature, 572: 230-234, https://doi.org/10.1038/s41586-019-1441-7, 2019.

Didan, K.: MOD13Q1 MODIS/Terra Vegetation Indices 16-Day L3 Global 250m SIN Grid V006. NASA EOSDIS Land Processes DAAC. https://doi.org/10.5067/MODIS/MOD13Q1.006, 2015.

Didane, D. H., Rosly, N., Zulkafli, M. F., and Shamsudin, S. S.: Evaluation of wind energy potential as a power generation source in Chad. International Journal of Rotating Machinery, vol. 2017, Article ID 3121875, 10 pp, 2017.

Do, F. and Rocheteau, A.: Cycle annuel de transpiration d'Acacia raddiana par la mesure des flux de sève brute (Nord-Sénégal). In Un arbre au désert : Acacia raddiana (pp. 119–142). Paris, (2003).

Do, F. C., Rocheteau, A., Diagne, A. L., Goudiaby, V., Granier, A., and Lhomme, J. P.: Stable annual pattern of water use by Acacia tortilis in Sahelian Africa. Tree Physiology, 28(1), 95–104. https://doi.org/10.1093/treephys/28.1.95, 2008.

Edmunds, W. M. and Gaye, C.B.: Estimating the spatial variability of groundwater recharge in the Sahel using chloride. J. Hydrol., 156(1-4):47-59, 1994.

Edmunds, W. M., Fellman, E., and Goni, I. B.: Spatial and temporal distribution of groundwater recharge in northern Nigeria. Hydrogeology Journal, 10:205-215, 2002.

Feddes, R. A., Kowalik, P. J., and Zaradny, H.: Simulation of field water use and crop yield. Published in 1978 in Wageningen by Centre for agricultural publishing and documentation. Wageningen: Centre for Agricultural Pub. and Documentation. https://lib.ugent.be/catalog/rug01:000032129, 1978.

Fontes, J.-C., Maglione, G., and Roche, M.-A.: Données isotopiques préliminaires sur les rapports du lac Tchad avec les nappes de la bordure nord-est, Cah. Orstom. Hydrobiol., 6, 17– 34, 1969.

Fontes, J.-C., Gonfiantini, R., and Roche, M.-A. : Deuterium et oxygène-18 dans les eaux du Lac Tchad. Isotope Hydrology, IAEA-SM-129/23, 1970.

French, A. N., Hunsaker, D. J., and Thorp, K. R.: Remote sensing of evapotranspiration over cotton using the TSEB and METRIC energy balance models. Remote Sensing of Environment, 158, 281–294. https://doi.org/10.1016/J.RSE.2014.11.003, 2015.

Gebru, T.A. and Tesfahunegn, G.B.: Chloride mass balance for estimation of groundwater recharge in a semi-arid catchment of northern Ethiopia. Hydrogeology Journal, 27:363-378, 2019.

Global Soil Data Task Group: Global Gridded Surfaces of Selected Soil Characteristics (IGBP-DIS). ORNL DAAC, Oak Ridge, Tennessee, USA. https://doi.org/10.3334/ORNLDAAC/569, 2000.

Goni, I., Fellman, E., and Edmunds, W.: Rainfall geochemistry in the Sahel region of northern Nigeria, Atmos. Environ., 35, 4331– 4339, 2001.

https://doi.org/10.5194/hess-2021-390
Preprint. Discussion started: 30 July 2021

Griffis, T. J., Sargent, S. D., Lee, X., Baker, J. M., Greene, J., Erickson, M., Zhang, X., Billmark, K., Schultz, N., and Hu, N.: Determining the Oxygen Isotope Composition of Evapotranspiration Using Eddy Covariance. Boundary-Layer Meteorology, 137(2), 307–326. https://doi.org/10.1007/s10546-010-9529-5, 2010.

Groh, J., Stumpp, C., Lücke, A., Pütz, T., Vanderborght, J., and Vereecken, H.: Inverse estimation of soil hydraulic and transport parameters of layered soils from water stable isotopes and lysimeter data, Vadose Zone Journal 17:170168. Doi:10.2136/vzj2017.09.0168, 2018.

Harris, I., Osborn, T. J., Jones, P. and Lister, D.: Version 4 of the CRU TS monthly high-resolution gridded multivariate climate dataset. Sci Data 7, 109 (2020) https://doi.org/10.1038/s41597-020-0453-3

Isihoro, S., Matisoff, G., and Wehn, K.: Seepage relationship between Lake Chad and the Chad Aquifers, Groundwater, 34, 819– 826, 1996.

Hartig, F., Minunno, F., Paul, S.: BayesianTools: General-Purpose MCMC and SMC Samplers and Tools for Bayesian Statistics, 2019.

Jasechko, S., Sharp, Z. D., Gibson, J. J., Birks, S. J., Yi, Y., and Fawcett, P. J.: Terrestrial water fluxes dominated by transpiration, Nature, 496, 347–350, 2013.

Kool, D., Agam, N., Lazarovitch, N., Heitman, J. L., Sauer, T. J., and Ben-Gal, A.: A review of approaches for evapotranspiration partitioning. Agricultural and Forest Meteorology, 184, 56–70, 2014.

Lake Chad Basin Commission. (1993). Monitoring and management of groundwater resources in the Lake Chad Basin. Mapping of aquifers, water resources management, final report, R35985, Report BRGM R 35985 EA U/4S/93

Lake Chad Basin Commission. (2012). Report on the State of the Lake Chad Basin Ecosystem. http://www.cblt.org/sites/default/files/download_documents/report_on_the_state_of_the_lake_chad_basin_ecosystem.pdf

Leblanc, M.: Gestion des ressources en eau des grands bassins semi-arides à l'aide de la télédétection et des SIG: application à l'étude du bassin du lac Tchad, Afrique, PhD thesis, Université de Poitiers, Poitiers, 2002.

Leblanc, M., Favreau, G., Tweed, S., Leduc, C., Razack, M., and Mofor, l.: Remote sensing for groundwater modelling in large semiarid areas: Lake Chad basin, Africa. Hydrogeology Journal, 15(1), 97-100, 2007.

Lemoalle, J., Bader, J.-C., Leblanc, M., and Sedick, A.: Recent changes in Lake Chad: observations, simulations and management options (1973–2011), Global Planet. Change, 80, 247–254, 2012.

Lloyd, J. W.: A review of aridity and groundwater, Hydrological Processes, Vol. 1, 63-78, 1986.

Lloyd, J. W.: Groundwater in arid and semiarid regions. In: Silveira, L. and Usunoff E.J. [Eds.]: Groundwater (Vol. I), Encyclopedia of Life Support Systems, pp. 284–307, 2009.

Majnooni-Heris, A., Sadraddini, A. A., Nazemi, A. H., Shakiba, M. R., Neyshaburi, M. R., and Tuzel, I. H.: Determination of single and dual crop coefficients and ratio of transpiration to evapotranspiration for canola. Annals of Biological Research, 3(4), 1885–1894, 2012.

Mertens, J., Barkle, G. F., and Stenger, R.: Numerical analysis to investigate the effects oft he design and installation of equilibrium tension plate lysimeters on leachate volume, Vadose Zone Journal, 4:488-499, 2005.

https://doi.org/10.5194/hess-2021-390
Preprint. Discussion started: 30 July 2021

474 Millington, R. J. and Quirk, J. P.: Permeability of porous solids. Trans. Int. Congr. Soil Sci., 7(1), 97-106, 1961.
475 Mualem, Y.: A new model for predicting the hydraulic conductivity of unsaturated porous media, Water Resour. Res., 12,
476 513–522, doi:10.1029/WR012i003p00513, 1976.
477 Ngatcha, B. N., Mudry, J., and Leduc, C.: The state of understanding on groundwater recharge for the sustainable management
478 of transboundary aquifer in the Lake Chad basin, 2008.
479 Olivry, J., Chouret, A., Vuillaume, G., Lemoalle, J., and Bricquet, J.: Hydrologie du lac Tchad, Editions de l'ORSTOM, Paris
480 1996.
481 Palatella, L., Rana, G., and Vitale, D.: Towards a Flux-Partitioning Procedure Based on the Direct Use of High-Frequency
482 Eddy-Covariance Data. Boundary-Layer Meteorology, 153(2), 327–337. https://doi.org/10.1007/s10546-014-9947-x, 2014.
483 Richards, L. A.: Capillary conduction of liquids through porous mediums. Physics, 1(5), 318-333, 1931.
484 Righes, A. A.: Water uptake and root distribution of soybeans, grain sorghum and corn. Retrospective Theses and
485 Dissertations. Iowa State University, 1980.
486 Roche, M.: Tracage naturel salin et isotopique des eaux du systeme du Lac Tchad, These de Doctorat d'Etat, Travaux et
487 Documents de l'ORSTOM, ORSTOM (Office de la Recherche Scientifique et Technique d'Outre-Mer) editions, Paris, 1980.
488 Scanlon, B. R., Keese, K. E., Flint, A. L., Flint, L. E., Gaye, C. B., Edmunds, W. M., and Simmers. I.: Global synthesis of
489 groundwater recharge in semiarid and arid regions. Hydrol. Process. 20, 3335-3370, 2006.
490 Scanlon, T. M. and Sahu, P.: On the correlation structure of water vapor and carbon dioxide in the atmospheric surface layer:
491 A basis for flux partitioning. Water Resources Research, 44(10). https://doi.org/10.1029/2008WR006932, 2008.
492 Schaap, M. G., Leij, F. J., and van Genuchten, M. T.: ROSETTA: a computer program for estimating soil hydraulic parameters
493 with hierarchical pedotransfer functions, Journal of Hydrology, 251, 163-176, 2001.
494 Schenk, H. J. and Jackson, R. B.: Rooting depths, lateral root spreads and belowground aboveground allometries of plants in
495 water limited ecosystems. Journal of Ecology, 90, 480–494. https://doi.org/10.1046/j.1365-2745.2002.00682.x, 2002.
496 Shahrokhnia, M. H. and Sepaskhah, A. R.: Single and dual crop coefficients and crop evapotranspiration for wheat and maize
497 in a semi-arid region. Theoretical and Applied Climatology, 114(3–4), 495–510. https://doi.org/10.1007/s00704-013-0848-6,
498 2013.
499 Šimůnek, J., Sejna, M., Saito, H., Sakai, M., and van Genuchten, M. Th.: The HYDRUS-1D software package for simulating
500 the one-dimensional movement of water, heat, and multiple solutes in variably-saturated media, Version 4.15, Riverside,
501 California, 2009.
502 Sprenger, M., Volkmann, T. H. M., Blume, T., and Weiler, M.: Estimating flow and transport parameters in the unsaturated
503 zone with pore water stable isotopes, Hydrol. Earth Syst. Sci., 19(6), 2617-2635, doi:10.5197/hess-19-2617-2015, 2015.
504 Stumpp, C., Nützmann, G., Maciejewski, S., and Maloszewski, P.: A comparative modeling study of a dual tracer experiment
505 in a large lysimeter under atmospheric conditions, Journal of Hydrology, 375, 566-577, 2009.

https://doi.org/10.5194/hess-2021-390
Preprint. Discussion started: 30 July 2021

506 Stumpp, C., Stichler, W., Kandolf, M., and Šimůnek, J.: Effects of land cover and fertilization method on water flow and solute
507 transport in five lysimeters: a long-term study using stable water isotopes, Vadose Zone Journal, 11(1), doi:
508 10.2136/vzj2012.0075, 2012.
509 ter Braak, C.J.F., Vrugt, J.A.: Differential Evolution Markov Chain with snooker updater and fewer chains. Stat. Comput. 18,
510 435–446. https://doi.org/10.1007/s11222-008-9104-9, 2008.
511 Tewolde, D. O.: Investigating unsaturated zone water transport processes by means of biogeochemical analysis of soil depth
512 profiles: a comparative study of two semi-arid sites. M.Sc.-Thesis, Leibniz Universitaet Hannover, 2017.
513 Tewolde, D. O., Koeniger, P., Beyer, M., Neukum, C., Gröschke, M., Ronnelngar, M., Rieckh, H., and Vassolo, S.: Soil water
514 balance in the Lake Chad Basin using stable water isotope and chloride of soil profiles, Isotopes in Environmental & Health
515 Studies, submitted, 2019.
516 Tong, G. D., Liu, H. L., and Li, F. H.: Evaluation of dual crop coefficient approach on evapotranspiration calculation of cherry
517 trees. International Journal of Agricultural and Biological Engineering, 9(3), 29–39.
518 https://doi.org/10.3965/j.ijabe.20160903.1886, 2016.
519 Vanderborght, J. and Vereecken, H.: Review of dispersivity for transport modeling in soils, Vadose Zone Journal, 6(1), 29-52,
520 doi:20.2136/vzj2006.0096, 2007.
521 van Genuchten, M. T.: A close-form equation for predicting the hydraulic conductivity of unsaturated soils 1, Soil Science
522 Society of America Journal, 8(44), 892-898, 1980.
523 van Looy, K., Bouma, J., Herbst, M., Koestel, J., Minasny, B., Mishra, U., Montzka, C., Nemes, A., Pachepsky, Y. A.,
524 Padarian, J., and Schaap, M. G.: Pedotransfer functions in earth system science: challenges and perspectives, Reviews of
525 Geophysics, 55(4), 1199-1256, doi: 10.1002/2017RG000581, 2017.
526 Vassolo. S.: The aquifer recharge and storage systems to reduce the high level of evapotranspiration. In: Adaptive Water
527 Management in the Lake Chad Basin. World Water Week 09, FAO, pp. 30-44, 2009.
528 Vereecken, H., Javaux, M., Weynants, M., Pachepsky, Y. A., Schaap, M. G., and van Genuchten M. T.: Using pedotransfer
529 functions to estimate the van Genuchten-Mualem soil hydraulic properties: A review, Vadose zone Journal, 9(4), 759-820,
530 doi: 10.2136/vzj2010.0045, 2010.
531 Vereecken, H., Schnepf, A., Hopmans, J. W., Javaux, M., Or, D., Roose, T., … and Young, I. M.: Modeling soil processes:
532 Review, key challenges, and new perspectives, Vadose Zone Journal, 15(5), 1-57, doi: 10.2136/vzj.2015.09.0131, 2016.
533 Vieira, P. V. D., de Freitas, P. S. L., Ribeiro da Silva, A. L. B., Hashiguti, H. T., Rezende, R. and Junior, C. A. F.: Determination
534 of wheat crop coefficient (Kc) and soil water evaporation (Ke) in Maringa, PR, Brazil, African Journal of Agricultural, 11(44),
535 4551–4558. https://doi.org/10.5897/AJAR2016.11377, 2016.
536 Vuillaume, G.: Bilan hydrologique mensuel et modélisation sommaire du régime hydrologique du lac Tchad, Cahiers
537 ORSTOM. Série Hydrologie, 18, 23–72, 1981.

https://doi.org/10.5194/hess-2021-390
Preprint. Discussion started: 30 July 2021

Hydrology and Earth System Sciences
Discussions
Open Access
EGU

538 Wohlfahrt, G., Brilli, F., Hörtnagl, L., Xu, X., Bingemer, H., Hansel, A., and Loreto, F.: Carbonyl sulfide (COS) as a tracer
539 for canopy photosynthesis, transpiration and stomatal conductance: Potential and limitations. Plant, Cell and Environment,
540 35(4), 657–667. https://doi.org/10.1111/j.1365-3040.2011.02451.x, 2012.
541 Wu, Y., Du, T., Ding, R., Tong, L., and Li, S.: Multiple Methods to Partition Evapotranspiration in a Maize Field. Journal of
542 Hydrometeorology, 139–149. https://doi.org/10.1175/JHM-D-16-0138.1, 2016.
543 Zairi, R.: Étude géochimique et hydrodynamique du Bassin du Lac Tchad (la nappe phréatique dans les régions du Kadzell
544 (Niger oriental) et du Bornou (Nord-Est du Nigéria)), PhD thesis, Université de Montpellier 2, Montpellier, 2008.
545

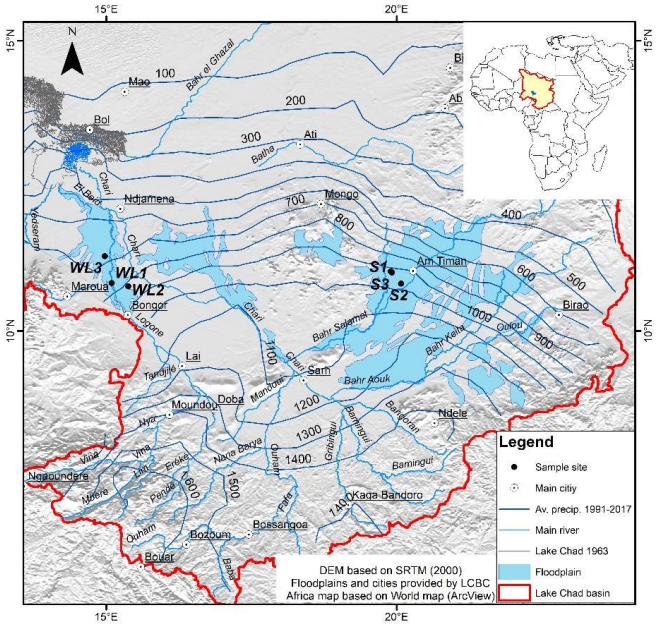

546

547 **Figure 1: Location of the six soil sampling sites within the Logone and Salamat river basins in the Lake Chad catchment. The map**
548 **inlet shows the location of the Lake Chad basin in Africa.**

https://doi.org/10.5194/hess-2021-390
Preprint. Discussion started: 30 July 2021

Hydrology and Earth System Sciences
Discussions

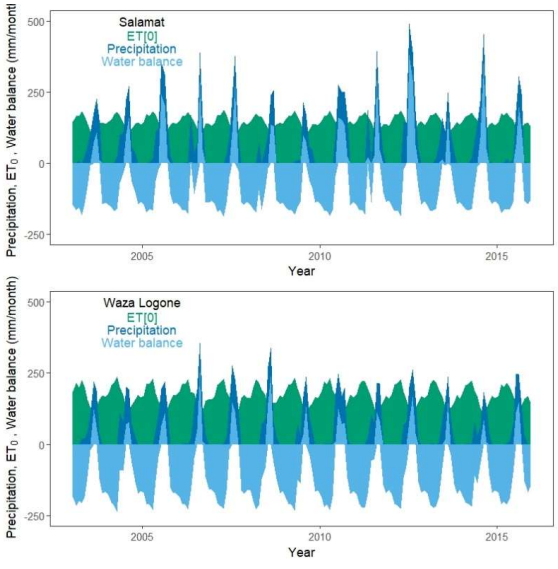

Figure 2: Monthly precipitation, reference evapotranspiration from the CRUTS 4 database (NCAR, 2017) and derived water balance for Salamat and Waza Logone.

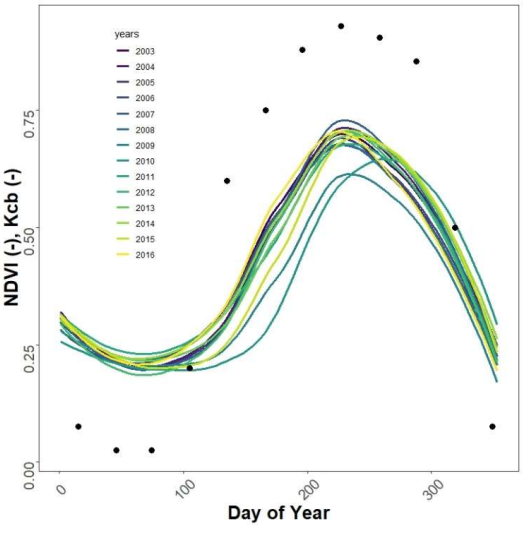

Figure 3: Average Normalized Difference Vegetation Index (NDVI, MODIS 16 day interval and 250 m spatial resolution) measured between 2003 and 2016 in the Salamat region and estimated monthly basal crop coefficient (Kcb, black points) for location S3.

https://doi.org/10.5194/hess-2021-390
Preprint. Discussion started: 30 July 2021

Hydrology and Earth System Sciences
Discussions

556

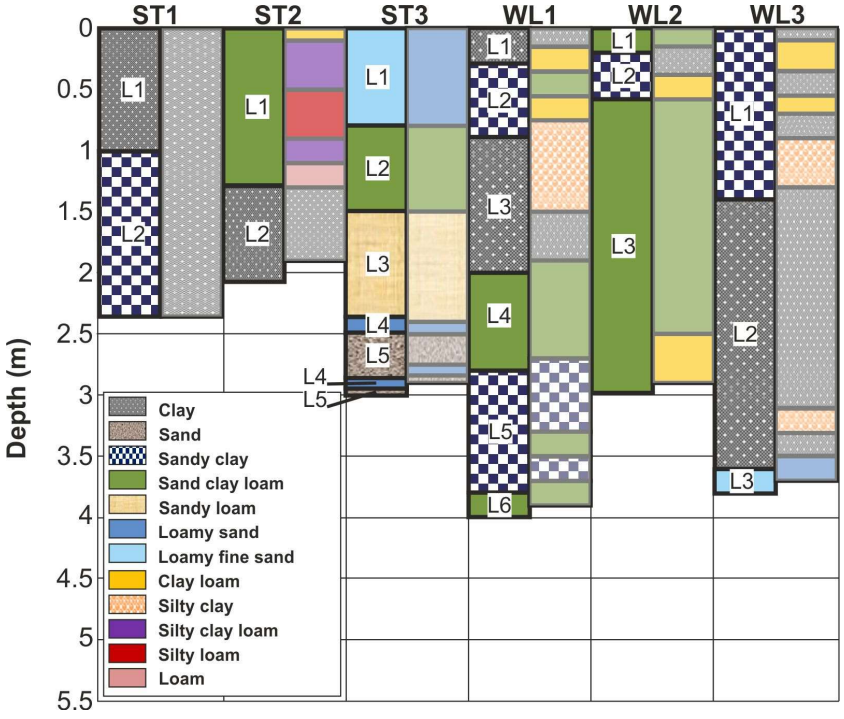

557

558 **Figure 4: Soil textures used in the model (left column) defined according to the grain size distribution analysis (right column) for**
559 **each of the six soil profiles.**

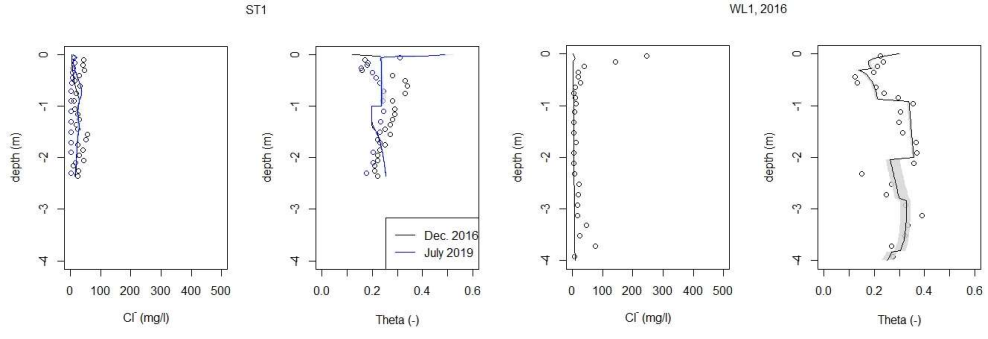

560

https://doi.org/10.5194/hess-2021-390
Preprint. Discussion started: 30 July 2021

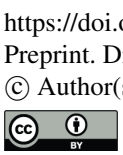

Hydrology and Earth System Sciences
Discussions

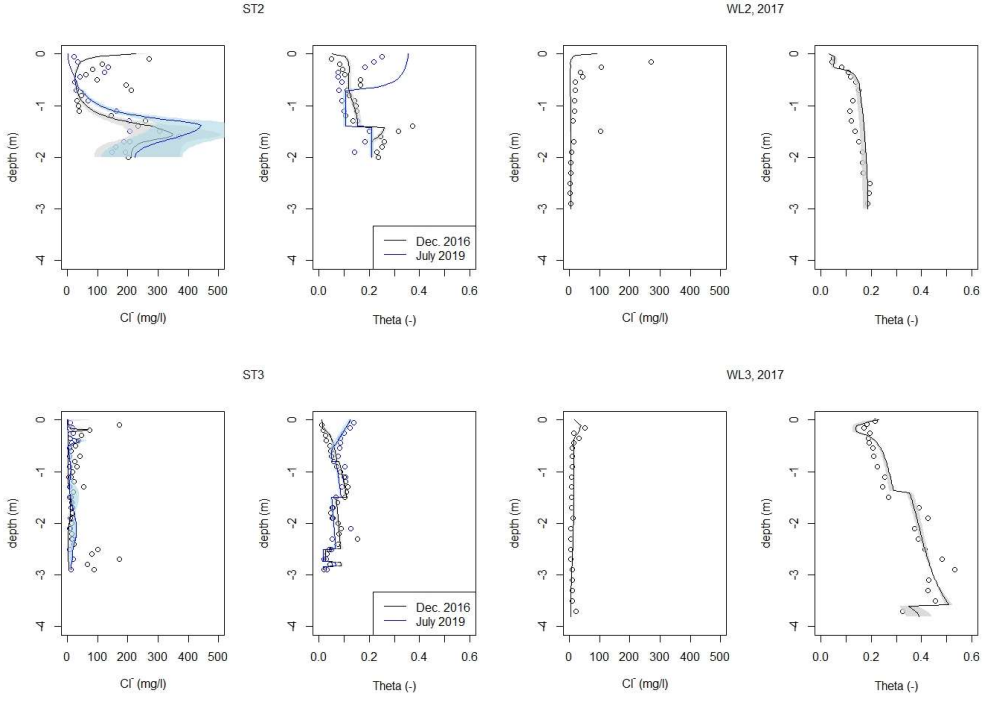

561

562

563 **Figure 5: Measured and simulated scenarios (for scenario definitions refer to Table 2) of chloride concentration and water content**
564 **for all six soil profiles. Obs: Observations.**

565

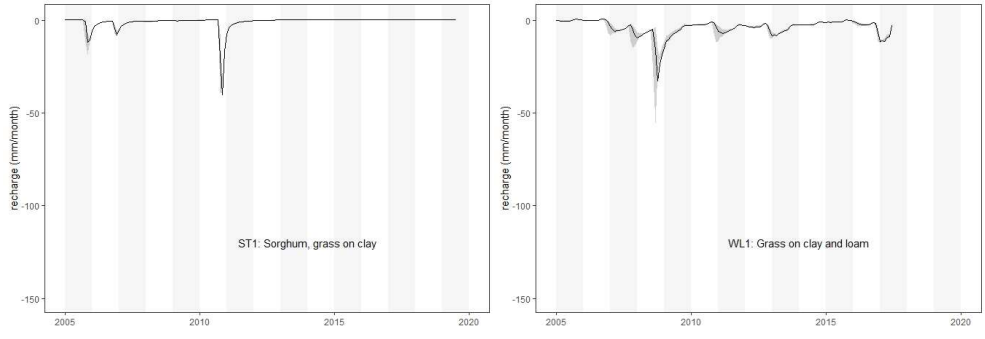

566

https://doi.org/10.5194/hess-2021-390
Preprint. Discussion started: 30 July 2021

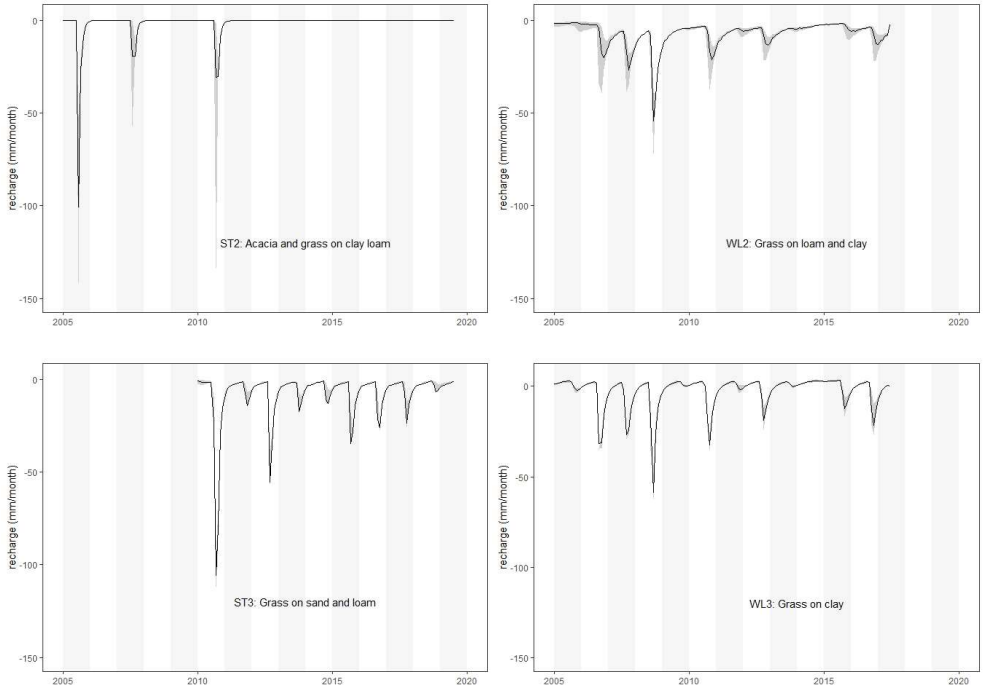

Figure 6: Calculated groundwater recharge for all scenarios and sampling locations with indication of vegetation and soil texture.

https://doi.org/10.5194/hess-2021-390
Preprint. Discussion started: 30 July 2021

Hydrology and Earth System Sciences
Discussions
Open Access
EGU

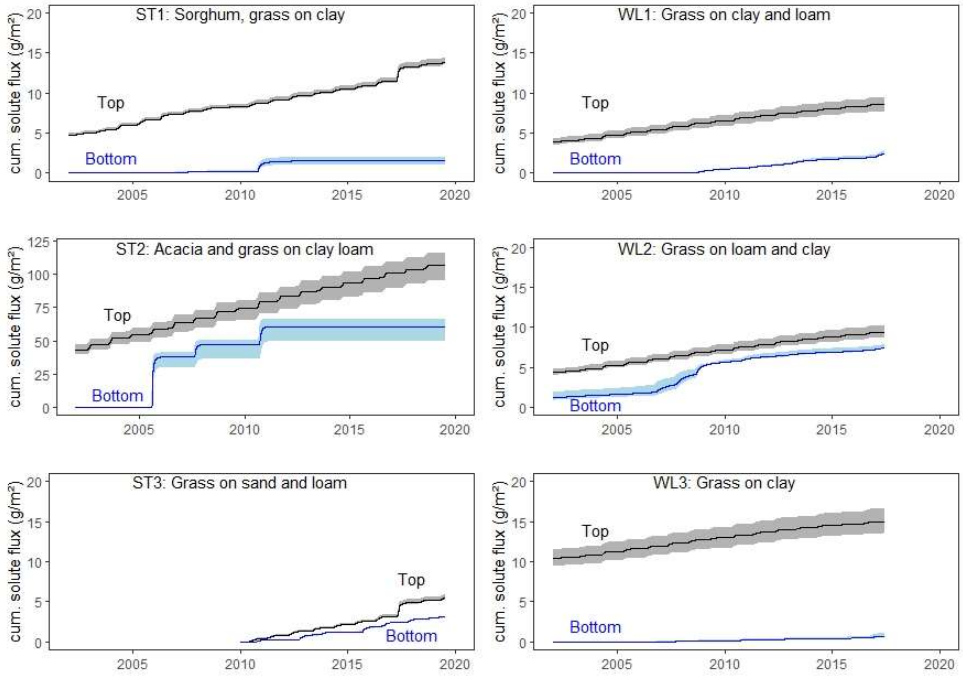

570

571 **Fig. 7: Cumulative solute flux on the upper and lower boundary of the models. The shaded areas represents the standard deviation**
572 **of 100 randomly selected model runs. Note the different y-axis scales between sites.**

https://doi.org/10.5194/hess-2021-390
Preprint. Discussion started: 30 July 2021

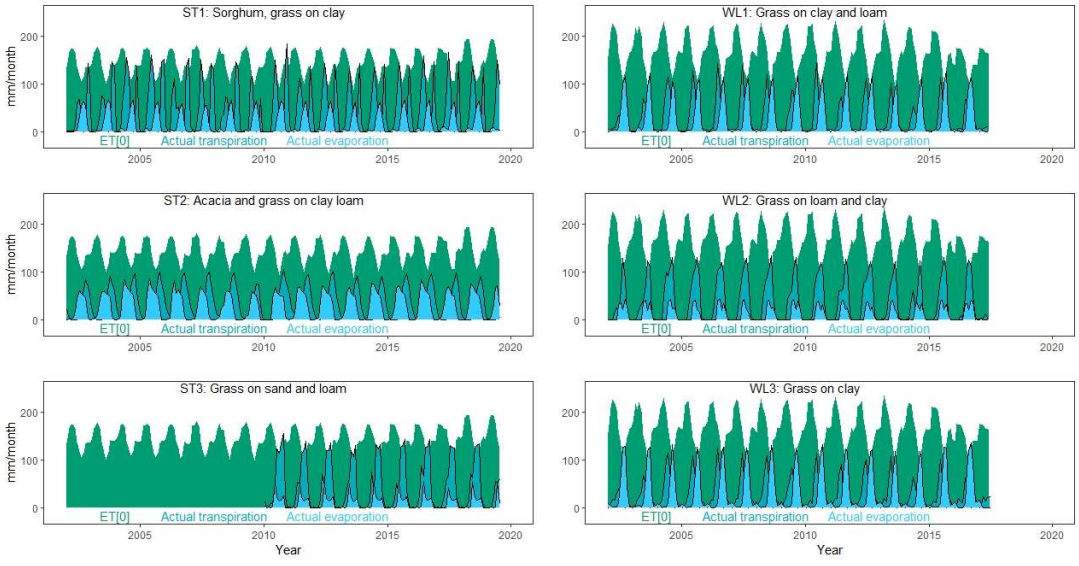

Fig. 8: Reference evapotranspiration from the CRUTS 4 database (NCAR 2017) as well as modelled average actual evaporation and transpiration of 100 randomly selected model runs.

Table 1: Names and geographic coordinates of the sampling locations with indication of average depth to groundwater.

Name	Location	Date of Sampling	Drilling depth (m)	Longitude (°)	Latitude (°)	Elevation (m a. s.l.)	Depth to Groundwater (m)
ST1	Gos Djarat	07-12-2016 11-07-2019	2.35 5.0	19.89644	11.02582	418	21
ST2	Kach Kacha	09-12-2016 16-07-2019	2.0 5.0	20.07473	10.81649	396	16-18
ST3	Gos Djarat	11-12-2016 13-07-2019	2.2 5.0	19.91687	11.00629	418	21
WL1	Katoa	01-06-2017	4.0	15.09235	10.82508	362	4
WL2	Loutou	01-06-2017	3.0	15.37817	10.76805	325	11-12
WL3	Zina	08-06-2017	3.8	14.97363	11.28858	304	3.6

https://doi.org/10.5194/hess-2021-390
Preprint. Discussion started: 30 July 2021

Hydrology and Earth System Sciences
Discussions

579 **Table 2: Crop evapotranspiration scenario used with the individual soil profiles.**

Scenario	Kcb	Ke	Root depth	Profile
Mean	average	average	average	All profiles
Min	minimum	minimum	average	All profiles
Min-RD	minimum	minimum	minimum	WL1
Mix-1	minimum	average	average	All profiles
Mix-2	average	minimum	average	ST1, WL2, WL3
Mix-3	maximum	average	average	ST3
Max	maximum	maximum	average	All profiles

580

581 **Table 3: Parametrization of water retention and unsaturated hydraulic conductivity functions according the Mualem-van**
582 **Genuchten model after Bayesian model calibration.**

Location	Texture	Depth (m)	θ_r (-)	θ_s (-)	α (m^{-1})	n (-)	K_s (md^{-1})
ST1	Clay	0-1	0.001	0.61±0.01	2.13±0.27	1.164±0.008	0.09±0.14
	Sandy clay	1-2.35	0.04	0.43±0.03	2.63±0.37	1.150±0.011	0.43±0.39
ST2	Sandy clay loam	0-1.4	0.04	0.38±0.02	1.18±0.08	1.36±0.047	0.03±0.16
	Clay	1.4 -2.1	0.07	0.48±0.08	2.66±0.36	1.203±0.052	0.11±0.28
ST3	Loamy fine sand	0-0.8	0.01	0.45±0.08	3.69±0.08	2.332±0.196	2.96±5.72
	Sandy clay loam	0.8-1.5	0.043	0.38±0.07	2.81±0.43	2.210±0.172	2.44±4.19
	Sandy loam	1.5-2.4	0.02	0.43±0.08	3.44±0.51	2.469±0.330	1.66±2.84
	Loamy sand	2.4-2.5	0	0.35±0.06	3.77±0.53	1.980±0.265	2.03±3.11
	Sand	2.5-2.75	0	0.34±0.04	3.73±0.53	2.730±0.372	5.42±8.86
	Loamy sand	2.75-2.84	0	0.35±0.06	3.77±0.53	1.980±0.265	2.03±3.11
	Sand	2.84-2.9	0	0.34±0.04	3.73±0.53	2.730±0.372	5.42±8.86
WL1	Clay	0-0.3	0.065	0.56±0.09	1.37±0.19	1.293±0.092	0.17±0.26
	Sandy clay	0.3-0.9	0.06	0.44±0.07	2.85±0.36	1.416±0.125	0.21±0.38
	Clay	0.9-2.0	0.103	0.42±0.03	1.55±0.21	1.187±0.065	0.19±0.42
	Sandy clay loam	2.0-2.8	0.075	0.49±0.07	2.34±0.33	1.598±0.227	0.13±0.28
	Sandy clay	2.8-3.8	0.081	0.43±0.06	2.60±0.35	1.266±0.134	0.09±0.19

https://doi.org/10.5194/hess-2021-390
Preprint. Discussion started: 30 July 2021

Hydrology and Earth System Sciences
Discussions

	Sandy clay loam	3.8-4.0	0.071	0.40±0.05	2.69±0.37	1.291±0.137	0.12±0.24
WL2	Sandy clay loam	0-0.2	0.03	0.41±0.07	3.22±0.45	1.502±0.151	0.30±0.57
	Sandy clay	0.2-0.6	0.01	0.37±0.06	2.56±0.39	1.422±0.081	0.09±0.19
	Sandy clay loam	0.6-3.0	0.01	0.37±0.03	1.39±0.19	1.566±0.06	0.10±0.10
WL3	Sandy clay	0-1.4	0.09	0.49±0.09	1.27±0.15	1.470±0.111	0.22±0.14
	Clay	1.4-3.6	0.105	0.53±0.05	2.03±0.29	1.285±0.100	0.17±0.36
	Loamy fine sand	3.6-3.8	0.056	0.39±0.08	2.90±0.45	1.789±0.293	1.23±2.40

Table 4: Average root mean square error (RMSE) and related standard deviation (SD) over all scenarios for water content (Theta) and chloride concentration.

	Theta (-)			Chloride concentration (mg/l)		
Location, Year	Average observation	Average simulation	Average RMSE	Average observation	Average simulation	Average RMSE
ST1, 2016/2019	0.25/0.22	0.23/0.23	0.06/0.04	30/6	18/22	19/19
ST2, 2016/2019	0.17/0.14	0.16/0.15	0.06/0.04	162/106	132/229	82/116
ST3, 2016/2019	0.06/0.08	0.07/0.06	0.02/0.02	42/10	6/13	58/10
WL1, 2017	0.27	0.27	0.05	31	6	59
WL2, 2017	0.13	0.15	0.02	40	3	117
WL3, 2017	0.31	0.33	0.04	12	13	9

Table 5: Calculated average annual recharge, fraction of recharge on average annual precipitation, standard deviations of recharge across the time-period 2005-2019 and 2005 – 2016 for Salamat and Waza Logone respectively.

Location	Average annual recharge (mm)	Fraction of average annual precipitation (%)	Standard deviation of annual recharge (mm)
ST1	7	0.9	17
ST2	9	1	29
ST3	93	12	69
WL1	28	4	32
WL2	54	8	46
WL3	6	1	48

https://doi.org/10.5194/hess-2021-390
Preprint. Discussion started: 30 July 2021

Hydrology and Earth System Sciences
Discussions
Open Access
EGU

589 **Table 6: Calculated average annual evaporation and transpiration and related standard deviations of 100 randomly accepted model**
590 **runs.**

Location	Average annual evaporation (mm)	Standard deviation of evaporation (mm)	Average annual transpiration (mm)	Standard deviations of transpiration (mm)	Average actual evapotranspiration (mm)
ST1	210	9	553	11	763
ST2	366	22	388	27	754
ST3	137	12	552	11	689
WL1	344	20	317	23	661
WL2	146	14	477	28	623
WL3	376	12	305	10	681

591